

# Receptor for advanced glycation end products up-regulation in cerebral endothelial cells mediates cerebrovascular-related amyloid $\beta$ accumulation after *Porphyromonas gingivalis* infection

曾, 凡

<https://hdl.handle.net/2324/4475037>





---

出版情報 : 九州大学, 2020, 博士 (学術), 課程博士  
バージョン :

権利関係 : © 2020 The Authors. This is an open access article under the terms of the Creative Commons Attribution-NonCommercial-NoDerivs License, which permits use and distribution in any medium, provided the original work is properly cited, the use is non-commercial and no modifications or adaptations are made.

## ORIGINAL ARTICLE

# Receptor for advanced glycation end products up-regulation in cerebral endothelial cells mediates cerebrovascular-related amyloid $\beta$ accumulation after *Porphyromonas gingivalis* infection

Fan Zeng<sup>1</sup>  | Yicong Liu<sup>2,3</sup> | Wanyi Huang<sup>1</sup> | Hong Qing<sup>4</sup>  | Tomoko Kadowaki<sup>5</sup> | Haruhiko Kashiwazaki<sup>6</sup> | Junjun Ni<sup>1,4</sup>  | Zhou Wu<sup>1,7</sup> 

<sup>1</sup>Department of Aging Science and Pharmacology, Kyushu University, Fukuoka, Japan

<sup>2</sup>The Affiliated Stomatology Hospital, School of Medical, Zhejiang University, Zhejiang, China

<sup>3</sup>Key Laboratory of Oral Biomedical Research of Zhejiang Province, School of Stomatology, Zhejiang University, Zhejiang, China

<sup>4</sup>Key Laboratory of Molecular Medicine and Biotherapy in the Ministry of Industry and Information Technology, Department of Biology, School of Life Science, Beijing Institute of Technology, Haidian District, Beijing, China

<sup>5</sup>Division of Frontier Life Science, Department of Medical and Dental Sciences, Graduate School of Biomedical Sciences, Nagasaki University, Nagasaki, Japan

<sup>6</sup>Section of Geriatric Dentistry and Perioperative Medicine in Dentistry, Division of Maxillofacial Diagnostic and Surgical Sciences, Faculty of Dental Science, Kyushu University, Fukuoka, Japan

<sup>7</sup>Faculty of Dental Science, OBT Research Center, Kyushu University, Fukuoka, Japan

## Correspondence

Zhou Wu, Department of Aging Science and Pharmacology, OBT Research Center,

## Abstract

Cerebrovascular-related amyloidogenesis is found in over 80% of Alzheimer's disease (AD) cases, and amyloid  $\beta$  ( $A\beta$ ) generation is increased in the peripheral macrophages during infection of *Porphyromonas gingivalis* (*P. gingivalis*), a causal bacterium for periodontitis. In this study, we focused on receptor for advanced glycation end products (RAGE), the key molecule involves in  $A\beta$  influx after *P. gingivalis* infection to test our hypothesis that  $A\beta$  transportation from periphery into the brain, known as " $A\beta$  influx," is enhanced by *P. gingivalis* infection. Using cultured hCMEC/D3 cell line, in comparison to uninfected cells, directly infection with *P. gingivalis* (multiplicity of infection, MOI = 5) significantly increased a time-dependent RAGE expression resulting in a dramatic increase in  $A\beta$  influx in the hCMEC/D3 cells; the *P. gingivalis*-up-regulated RAGE expression was significantly decreased by NF- $\kappa$ B and Cathepsin B (CatB)-specific inhibitors, and the *P. gingivalis*-increased  $I\kappa$ B $\alpha$  degradation was significantly decreased by CatB-specific inhibitor. Furthermore, the *P. gingivalis*-increased  $A\beta$  influx was significantly reduced by RAGE-specific inhibitor. Using 15-month-old mice (C57BL/6JMsSlc, female), in comparison to non-infection mice, systemic *P. gingivalis* infection for three consecutive weeks ( $1 \times 10^8$  CFU/mouse, every 3 days, intraperitoneally) significantly increased the RAGE expression in the CD31-positive endothelial cells and the  $A\beta$  loads around the CD31-positive cells in the mice's brains. The RAGE expression in the CD31-positive cells was positively correlated with the  $A\beta$  loads. These observations demonstrate that the up-regulated RAGE expression in cerebral

**Abbreviations:** AD, Alzheimer's disease; APP, amyloid precursor protein;  $A\beta$ , amyloid  $\beta$  protein; BBB, blood-brain barrier; BMDM, bone marrow-derived macrophages; BSA, bovine serum albumin; C3, complement component 3; C5, complement component 5; CatB, cathepsin B; CD31, cluster of differentiation 31; CFU, colony-forming unit; CLMS, confocal laser microscope system; hCMEC/D3, human cerebral microvascular endothelial cell line; HRP, horseradish peroxidase; ICLAC, International Cell Line Authentication Committee;  $I\kappa$ B $\alpha$ , nuclear factor of kappa light polypeptide gene enhancer in B-cell inhibitor, alpha; LPS, lipopolysaccharide; LRP1, low-density lipoprotein receptor-related protein1; MOI, multiplicity of infection; Na-F, sodium fluorescein; NF- $\kappa$ B, nuclear factor kappa-light-chain-enhancer of activated B cells; PBS, phosphate buffer saline; PCR, polymerase chain reaction; PFA, paraformaldehyde; *P. gingivalis*, *porphyromonas gingivalis*; P $\beta$ LPS, lipopolysaccharide from *P. gingivalis*; p $I\kappa$ B $\alpha$ , phosphorylated  $I\kappa$ B $\alpha$ ; RAGE, advanced glycation end products; RRID, Research Resource Identifier (see scicrunch.org); SDS-PAGE, sodium dodecyl sulfate-polyacrylamide gel electrophoresis; TBS, tris-buffered saline; TLR2, toll-like receptor 2; TLR4, toll-like receptor 4.

This is an open access article under the terms of the Creative Commons Attribution-NonCommercial-NoDerivs License, which permits use and distribution in any medium, provided the original work is properly cited, the use is non-commercial and no modifications or adaptations are made.

© 2020 The Authors. *Journal of Neurochemistry* published by John Wiley & Sons Ltd on behalf of International Society for Neurochemistry

Faculty of Dental Science, Kyushu University, Fukuoka 812-8582, Japan.  
Email: zhouw@dent.kyushu-u.ac.jp

Junjun Ni, Key Laboratory of Molecular Medicine and Biotherapy in the Ministry of Industry and Information Technology, Department of Biology, School of Life Science, Beijing Institute of Technology, Haidian District, Beijing 100081, China.  
Email: nijunjun@bit.edu.cn

#### Funding information

Japanese KAKENHI Grants-in-Aid for Scientific Research, Grant/Award Number: JP16K11478 and JP17K17093; Research grant for OBT research center from Kyushu University

endothelial cells mediates the A $\beta$  influx after *P. gingivalis* infection, and CatB plays a critical role in regulating the NF- $\kappa$ B/RAGE expression.

#### KEYWORDS

amyloid  $\beta$ , cathepsin B, cerebral endothelial cells, NF- $\kappa$ B, *Porphyromonas gingivalis*, receptor for advanced Glycation end products

## 1 | INTRODUCTION

Alzheimer's disease (AD), the most common cause of dementia, affects more than 50 million people worldwide. The prevalence of AD continues to grow because of the increase in the aging population (Hodson, 2018). As the major pathological marker of AD brain, amyloid  $\beta$  protein (A $\beta$ ), a polypeptide consisting of 39–43 acid residues, is proteolytically generated by cleavage of amyloid precursor protein (Chen et al., 2019). A $\beta$  accumulation in and around the cerebral vasculature, known as cerebral amyloid angiopathy (CAA), has been found in more than 80% of AD patients (Kovari, Herrmann, Hof, & Bouras, 2013).

Brain A $\beta$  in AD has long been thought to be generated in the brain itself by neurons; however, A $\beta$  was recently found to be generated peripherally by platelets, skeletal muscle cells, skin fibroblasts, and monocyte/macrophages (Evin, Zhu, Holsinger, Masters, & Li, 2003; Kuo et al., 2000; Nie et al., 2019; Roher & Kokjohn, 2009). Recent studies have also shown that peripheral A $\beta$  can be transferred into the brain using a model of parabiosis between APP<sup>swe</sup>/PS1<sup>dE9</sup> transgenic AD mice and their wild-type littermates, which thus determines the human A $\beta$  originating from transgenic AD model mice in the circulation and CAA in the brains of wild-type mice after a 12-month period of parabiosis (Bu et al., 2018).

The physical and functional integrity and health of the mammalian brain are basically maintained by the blood–brain barrier (BBB), which is specialized to prevent pathogens and circulating cells from entering the brain and causing damage. Cerebral endothelial cells are part of the BBB, connected by tight junctions that function as a “physical barrier” and prevent molecular traffic between the blood and brain (Iadecola, 2013). Cerebral endothelial cells also act as a “transport barrier” because of the presence of specific transport systems regulating the transcellular traffic of small molecules (Abbott, Ronnback, & Hansson, 2006). Regarding A $\beta$  transportation in the cerebral endothelial cells, low-density lipoprotein receptor-related protein 1 (LRP1) is the receptor for A $\beta$  transport from the brain to the peripheral blood (A $\beta$  efflux), while receptor for advanced glycation end products (RAGE) is accepted as the

receptor for A $\beta$  transport from the peripheral blood to the brain (A $\beta$  influx) (Deane et al., 2003; Sagare, Deane, & Zlokovic, 2012). RAGE up-regulation has been found in the brains of both AD patients and AD mouse models, suggesting that RAGE is involved in the pathological A $\beta$  accumulation in the AD brain (Miller et al., 2008; Du Yan et al., 1996).

Numerous clinical studies have shown that periodontitis, a common oral infection disease, is positively linked to cognitive decline in elderly people (Noble et al., 2009; Sparks Stein et al., 2012) as well as AD patients (Ide et al., 2016). Furthermore, the components of *Porphyromonas gingivalis*, a key pathogen involved in periodontitis, including lipopolysaccharide (LPS) and gingipain, have been found in human AD brains (Dominy et al., 2019; Poole, Singhrao, Kesavalu, Curtis, & Crean, 2013). These findings suggest the influence of periodontitis on the AD onset as well as its pathological processing.

We previously showed that chronic exposure to LPS from *P. gingivalis* induced CatB-dependent AD-like phenotypes that included memory impairment, microglia-mediated neuroinflammation and intracellular A $\beta$  accumulation in neurons of middle-aged mice (Wu et al., 2017). Furthermore, other researchers have found that oral infection with *P. gingivalis* induced A $\beta$  formation in the brain of adult mice (Ilievski et al., 2018). However, the role of A $\beta$  accumulation in the brain during systemic *P. gingivalis* infection remains unclear.

*P. gingivalis* has been recognized as a keystone pathogen for periodontitis because it is a master evader of the host's immune system (Bielecka et al., 2014; Reife et al., 2006). *P. gingivalis* is resistant to destruction by complements that are dependent on gingipains degrading complement 3 (C3) and C5, thereby preventing the deposition of C3b and C5a on the surface of *P. gingivalis* (Slaney, Gallagher, Aduse-Opoku, Pell, & Curtis, 2006). The immune evasion strategies of *P. gingivalis* prolong its stay in the systemic circulation, providing more opportunities for this bacterium to make direct contact with cerebral endothelial cells. We recently demonstrated the generation of A $\beta$  in the inflammatory monocytes/macrophages in the gingival tissues of periodontitis patients and in the liver of middle-aged mice after chronic systemic *P. gingivalis* infection, indicating that the peripheral

pools of A $\beta$  expand during chronic systemic *P. gingivalis* infection (Nie et al., 2019).

In this study, we tested our hypothesis that RAGE in cerebral endothelial cells contributes to the peripheral A $\beta$  influx during chronic *P. gingivalis* infection, adding new insight into the influence of systemic periodontal bacterial infection on AD.

## 2 | MATERIALS AND METHODS

All reagents in this study were purchased within 2 years and stored properly according to the manufactures. All experiments were performed and repeated according to the same time schedule. The study was not pre-registered. The study was exploratory. The experimenters were not blinded to experimental condition.

### 2.1 | Animals

Fifteen-month-old female mice (C57BL/6JmsSlcJapan SLC, Incorporation, MGI Cat# 5658738, RRID:MGI:5658738) were kept in a pathogen-free condition at the Kyushu University Faculty of Dental Sciences. All animal experiments were conducted in accordance to the protocols approved by the Animal Care and Use Committee of Kyushu University (A27-232-0). The mice ( $n = 6$ ) were intraperitoneally injected with *P. gingivalis* ( $1 \times 10^8$  CFU/mouse) in 100  $\mu$ L phosphate-buffered saline (PBS) every 3 days and last for three consecutive weeks. The age-matched control mice ( $n = 6$ ) were injected with 100  $\mu$ L PBS in the same time course. Then the mice were anesthetized via an intraperitoneal injection of widely used somnopentyl (50 mg/kg Kyoritsu Seiyaku Cat# 7212101) and sacrificed by cardiac perfusion with PBS followed by 4% paraformaldehyde, and then the brain samples were collected immediately. The active ingredient of somnopentyl is pentobarbital sodium, which binds to the gamma-aminobutyric acid-A receptor and causes central nervous system depression (Luo et al., 2015). We fixed three mice per group for immunostaining in this study. The sample size determination was based on the behavior test data of our previously publication (Wu et al., 2017). G\*Power software (G\*Power 3.1.9.7, means: difference between two independent means, two tails) was used to verify the Power of the behavior test (Charan & Kantharia, 2013). The  $\alpha$  err prob was set at 0.05, and the sample size of each group was 6. The effect size  $d$  was 5.6537 which was determined by mean and SD of the two groups (group 1: mean 300, SD 1; group 2: mean 180, SD 30). As the Power was 1 after calculation, six mice in each group were used for the behavior test in this study.

### 2.2 | Step-through passive avoidance test

The step-through passive avoidance test was used to test memory decline in this paper. The device included a bright compartment and a dark compartment with an electrifiable grid floor, which were separated by a sliding door. In acquisition phase, each mouse was placed

in the bright compartment and was able to freely explore for 30 s. After the door was opened, mice entered into the dark compartment. Then the door was closed and an electric shock (0.2 mA, 2 s) was delivered through the grid. The endpoint of the acquisition phase was that mice stay in the bright compartment for 300 s without entering the dark compartment. From the first day of *P. gingivalis* injection, the step-through passive avoidance test was carried out every 7 days until 3 weeks after *P. gingivalis* injection. The latency was set up to 300 s and no electric shock was given. To minimize animal pain in procedures, the mice were gently picked out from or put back to their cages, and were returned to their familiar environment as soon as possible after behavior test or injection. No other procedures involved animal pain, suffering or distress. Mice failed to enter the dark compartment would be excluded, but no mouse was excluded or died during experiments.

### 2.3 | Cell culture

The hCMEC/D3 cell line (Millipore Cat# SCC066, RRID:CVCL\_U985) was maintained in EBM-2 medium with supplements (Lonza Cat# CC-3202) and grown to confluence in rat-tail collagen type I coated cell culture dishes at 37°C and 5% CO<sub>2</sub> in humid atmosphere. The hCMEC/D3 was infected by *P. gingivalis* (ATCC33277, MOI (multiplicity of infection) = 5) for indicated time points. For the immunofluorescent staining, the number of hCMEC/D3 was  $5 \times 10^4$  and the corresponding number of *P. gingivalis* was  $2.5 \times 10^5$ . For the real-time quantitative polymerase chain reaction (PCR) analysis and immunoblotting analysis, the number of hCMEC/D3 was  $1 \times 10^6$  and the corresponding number of *P. gingivalis* was  $5 \times 10^6$ . For the Na-F permeability and A $\beta_{1-42}$  transportation, the number of hCMEC/D3 was  $7 \times 10^5$  and the corresponding number of *P. gingivalis* was  $3.5 \times 10^6$ . All the inhibitors were added 1 hr before *P. gingivalis* infection. The maximum number of passages for the hCMEC/D3 cell line was 30 passages. The cell line was last authenticated in 2018 by the supplier and this cell line is not listed as a commonly misidentified cell line by the ICLAC.

### 2.4 | Bacterial strain and culture conditions

*P. gingivalis* ATCC33277 was maintained on blood agar plate containing 40 mg/mL Tryptone-Soya Agar (Nissui Cat# 05516), 5 mg/mL Brain Heart Infusion (Becton Dickinson Cat# 211059), 1 mg/mL L-Cysteine Hydrochloride (Wako Cat#039-05274), 1  $\mu$ g/mL Menadione (Sigma-Aldrich Cat# M9429-25G), 5  $\mu$ g/mL Hemin (Sigma-Aldrich Cat# 51280-1G) and 5% defibrinated sheep blood (ThermoFisher Cat# R54020). When *P. gingivalis* was ready to use, it was grown in liquid medium containing 37 mg/mL Brain Heart Infusion, 2.5 mg/mL Yeast Extract (Becton Dickinson Cat# 212750), 1 mg/mL Cysteine, 1  $\mu$ g/mL Menadione and 5  $\mu$ g/mL Hemin. We used an anaerobic chamber with 10% CO<sub>2</sub>, 10% H<sub>2</sub>, and 80% N<sub>2</sub> maintaining at 37°C for *P. gingivalis* culture. Before *P. gingivalis* infection, the liquid medium was centrifuged (6,000 g, 10 min) and replaced by EBM-2 medium without antibiotics.

## 2.5 | Immunofluorescent staining

For the hCMEC/D3 cells staining, cells were fixed with 4% Formaldehyde solution (Sigma-Aldrich Cat# 11-0720-5) for 1 hr at 4°C, and permeated with 0.1% Triton X-100 (Sigma-Aldrich Cat# 30-5140-5) for 5 min at 25°C. After blocking with 3% Albumin from Bovine Serum (BSA) (Wako Cat# 017-21273) in PBS, the cells were incubated with goat anti-RAGE (1:1,000; R&D Systems Cat# AF1179, RRID:AB\_354649) or rabbit anti-p65 (1:1,000; Abcam Cat# ab16502, RRID:AB\_443394) at 4°C overnight. After washing with PBS for three times, the cells were then incubated with donkey anti-goat Alexa Fluor 488 (1:1,000; Jackson ImmunoResearch Labs Cat# 705-545-147, RRID:AB\_2336933) or donkey anti-rabbit Alexa Fluor 488 (1:1,000; Jackson ImmunoResearch Labs Cat# 711-545-152, RRID:AB\_2313584) at 4°C for 2 hr. After washing with PBS for three times, cell nuclear were stained with Hoechst (1:1,000; Sigma-Aldrich Cat#14533) for 5 min and mounted in Vectashield anti-fading medium (Vector Laboratories Cat# H-1000, RRID:AB\_2336789). In the case of F-actin staining, Texas Red™-XPhalloidins (Invitrogen Cat# T7471) were used at the recommended concentration for 2 hr at 4°C.

The brain samples of mice were cut into serial coronal frozen sections (10 µm) ( $n = 3$  in each group). Then the sections were incubated with 3% BSA in PBS containing 0.1% Triton X-100 for 1 hr at 25°C. After that, 0.05% Sudan Black B (Sigma-Aldrich Cat# 199664-25G) was used to block non-specific staining. Then the sections were incubated with goat anti-CatB (1:1,000; Santa Cruz Biotechnology Cat# sc-6493, RRID:AB\_2086939), rabbit anti-p65, goat anti-RAGE, rabbit anti- $\text{A}\beta_{1-42}$  (1:1,000; Thermo Fisher Scientific Cat# 44-344, RRID:AB\_2533636), and rat anti-CD31 (1:1,000; BD Biosciences Cat# 553370, RRID:AB\_394816) at 4°C overnight. After washing with PBS for three times, the sections were then incubated with donkey anti-goat Alexa Fluor 488 (1:1,000; Jackson ImmunoResearch Labs Cat# 705-545-147, RRID:AB\_2336933) and donkey anti-rat Cy3 (1:1,000; Jackson ImmunoResearch Labs Cat# 712-165-153, RRID:AB\_2340667) at 4°C for 2 hr. After washing with PBS for three times, the sections were stained with Hoechst for 5 min and mounted in Vectashield anti-fading medium. Fluorescence images were taken using a CLMS (2si Confocal Laser Microscope, Nikon).

## 2.6 | Real-time quantitative PCR analysis

The mRNA was isolated from hCMEC/D3 cell cultures after stimulation with *P. gingivalis*, or pre-treatment with Bay11-7082 (10 µM; Sigma-Aldrich Cat#B5556-10MG), SN50 (20 µM; Sigma-Aldrich Cat#SML1471-1MG) or CA-074Me (10 µM; Peptide Cat# 4323-v), respectively, with RNAiso Plus (Takara Cat# 9109) under the manufacturer's instructions. And then up to 1 µg of extracted mRNA was reverse transcribed to cDNA using the QuantiTect Reverse Transcription Kit (Qiagen Cat# 205314). The cDNA was amplified in duplicate using a Rotor-Gene SYBR Green RT-PCR Kit (Qiagen Cat#204174) with a

Corbett Rotor-Gene RG-3000A Real-Time PCR System. The data were evaluated using the RG-3000A software program (version Rotor-Gene 6.1.93 Corbett). The sequences of primer pairs were as follows: human RAGE, forward 5'-CCAGGAGGAAGAGGAGGAG-3' and reverse 5'-GCTGATGGATGGGATCTGTC-3'; human CatB, forward 5'-AACACGTCACCGGAGAGATGA-3' and reverse 5'-CCCAGTCAGTGTTCCAGGAGTT-3'; human TLR2, forward 5'-GCCAAAGTCTTGA TTGATTGG-3' and reverse 5'-TTGAAGTTCTCCAGCTCCTG-3'; human TLR4, forward 5'-TACAAAATCCCGACAACCTCC-3' and reverse 5'-GCTGCCTAAATGCCTCAGGG-3'; human Actin, forward 5'-CATC TCTTGCTCGAAGTCCA-3' and reverse 5'-ATCATGTTTGAGACCTT CAACA-3'.

## 2.7 | Immunoblotting analysis

The hCMEC/D3 cells were grown to confluence and were harvested after *P. gingivalis* infection for indicated time points, and protein was extracted after harvesting samples. For the nuclear lysate, cells were harvested and nuclear were isolated using the Nuclear Extraction Kit (AbcamCat#ab113474). Each sample was homogenized and separated using 12% SDS-PAGE gel. After electrophoresis, the proteins were transferred to nitrocellulose membranes. After blocking with 5% milk in TBS, the membranes were incubated with primary antibodies at 4°C overnight. The primary antibodies were as follows: rabbit anti-RAGE (1:1,000; Abcam Cat# ab3611, RRID:AB\_303947); rabbit anti-p65; goat anti-CatB (1:1,000; Santa Cruz Biotechnology Cat# sc-6493, RRID:AB\_2086939); rabbit anti- $\text{I}\kappa\text{B}\alpha$  (1:1,000; Cell Signaling Technology Cat# 8993, RRID:AB\_2797687); mouse anti- $\text{pI}\kappa\text{B}\alpha$  (1:1000; Cell Signaling Technology Cat# 9246, RRID:AB\_2267145); and rabbit anti-Lamin B1 (1:1,000, Cell Signaling Technology Cat# 13435, RRID:AB\_2737428). After washing, the membranes were incubated with HRP-labeled second antibodies and mouse anti-actin (1:1,000; Abcam Cat# ab20272, RRID:AB\_445482) at 25°C for 2 hr. The second antibodies were as follows: anti-rabbit (1:1,000; GE Healthcare Cat#NA934V), anti-goat (1:1,000; R&D Systems Cat# HAF109, RRID:AB\_357236), and anti-mouse (1:1,000; GE Healthcare Cat#NA931V). Finally, the membrane-bound, HRP-labeled antibodies were detected by an Immobilon ECL Ultra Western HRP Substrate (Millipore Cat#WBULS0100) with an image analyzer (LAS-1000 Fuji Photo Film).

For the secreted CatB, culture medium was collected after *P. gingivalis* infection for indicated time points. The medium was centrifuged to pellet cell debris at 750 g for 5 min. Then supernatant was collected and protein concentration was determined. The loading quantity of each sample was 10 µg and the following procedures were the same as above.

## 2.8 | Na-F permeability

The permeability of endothelial monolayer was determined using Sodium Fluorescein (Na-F) (100 ng/mL; Sigma-Aldrich Cat# F6377). The transcytosis system was constructed by confluence hCMEC/



D3 cells on inserts with collagen-coated polycarbonate transwell membrane filters (cell culture inserts; Millicell Cell Culture Inserts, RRID:SCR\_015799). The hCMEC/D3 monolayer was cultured in the apical side of a 24-well tissue culture insert. The EBM-2 medium was added into both the apical side and the basolateral side. After *P. gingivalis* infection at the apical side for 12 hr, all EBM-2 medium was replaced by warmed Assay Buffer. Fluorescence labeled Na-F was added into the apical Assay Buffer, after 5 min, inserts were removed and the fluorescence of the basolateral Assay Buffer was determined by a reader (infiniteM200 TECAN, excitation wavelength, 485 nm; measurement wavelength, 535 nm). These experiments were carried out at 37°C.

## 2.9 | A $\beta_{1-42}$ transportation

The transcytosis system was the same with Na-F permeability experiment. After *P. gingivalis* infection at the apical side for 12 hr, all EBM-2 medium was replaced by warmed Assay Buffer. Thirty minutes after adding HiLyte Fluor 488-labeled A $\beta_{1-42}$  (50 nM; AnaSpec Cat#AS-60479-01) into the apical side, inserts were removed and the fluorescence of the basolateral Assay Buffer was determined by the reader (infiniteM200 TECAN, excitation wavelength, 485 nm; measurement wavelength, 535 nm). The RAGE-specific inhibitor FPS-ZM1 (10  $\mu$ M; Abcam Cat#ab235552) was added 1 hr before *P. gingivalis* infection. These experiments were carried out at 37°C. For the A $\beta_{1-42}$  transportation and Na-F permeability, the following calculation was used:  $P [\text{cm/s}] = V_D / (A \times M_D) \times (\Delta M_R / \Delta t)$ . Where  $V_D$  is the apical side volume,  $A$  is the membrane surface area,  $M_D$  is the apical amount, and  $\Delta t$  is the time and  $\Delta M_R$  is deduced from a standard curve (Di Marco et al., 2019).

## 2.10 | Statistical analyses

The data are represented as the means  $\pm$  SEM. All data presented represent the mean of at least three replicates of independent cell culture preparations. The statistical analyses were performed by one-way ANOVA, two-way ANOVA, Student's *t* test, or multiple *t* test using the GraphPad Prism software package (GraphPad Software 7.00). A value of  $p < .05$  was considered to indicate statistical significance. Normality was determined using the Shapiro-Wilk normality test. There is no test for outliers and no data point was excluded.

## 3 | RESULTS

### 3.1 | RAGE expression was up-regulated in hCMEC/D3 cells after *P. gingivalis* infection

We used the hCMEC/D3 cell line because it has been extensively characterized for the brain endothelial phenotype and is a model of

the human BBB function. The time course of in vitro experiments was set up to 12 hr after *P. gingivalis* infection, as *P. gingivalis* can be kept alive for up to 12 hr in our culture system (Liu et al., 2017; Nie et al., 2019). Compared with the uninfected cells (None group), the mRNA expression of RAGE was significantly increased in the hCMEC/D3 cells from 3 hr (two-fold) to 12 hr (2.8-fold) after *P. gingivalis* infection (Figure 1a), the protein expression of RAGE in hCMEC/D3 cells was significantly increased from 6 to 12 hr after *P. gingivalis* infection (Figure 1b and c), and the immunofluorescent density of RAGE in hCMEC/D3 cells was significantly increased at 12 hr after *P. gingivalis* infection (Figure 1d and e). These observations showed that the RAGE expression in hCMEC/D3 cells was up-regulated after *P. gingivalis* infection.

### 3.2 | RAGE up-regulation in hCMEC/D3 cells was dependent on NF- $\kappa$ B activation after *P. gingivalis* infection

We next examined the involvement of the NF- $\kappa$ B signaling pathway in the RAGE expression in hCMEC/D3 cells after *P. gingivalis* infection. We focused on TLR2 and TLR4 as well as NF- $\kappa$ B activation in hCMEC/D3 cells after *P. gingivalis* infection because *P. gingivalis* activated NF- $\kappa$ B via TLR2 and TLR4 in bone marrow-derived macrophages (BMDMs) and RAW264.7 cells (Nie et al., 2019; Papadopoulos et al., 2017). Compared with uninfected cells, the mRNA expression of TLR2 in hCMEC/D3 cells was significantly increased at 3 hr (1.9-fold) and then returned to the baseline level from 6 to 12 hr after *P. gingivalis* infection (Figure 2a). In contrast, the mRNA expression of TLR4 in hCMEC/D3 cells was significantly increased from 6 hr (1.7-fold) to 12 hr (3.7-fold) after *P. gingivalis* infection (Figure 2a).

Nuclear extracts and cell lysates were prepared, and western blotting was conducted. The immunoreactivity of p65 in both with or without *P. gingivalis* infection groups were compared with corresponding Lamin B1, and then the relative immunoreactivity of the two groups was analyzed with two-way ANOVA. After analysis, we found that the translocation of p65 into the nucleus of hCMEC/D3 cells was significantly increased at 1 and 3 hr and lasting until 12 hr after *P. gingivalis* infection (Figure 2b and c). The *P. gingivalis* infection-induced increase in nuclear p65 localization in hCMEC/D3 cells was further confirmed by immunofluorescent staining (Figure 2d).

We further examined the phosphorylation and degradation of I $\kappa$ B $\alpha$  in hCMEC/D3 cells after *P. gingivalis* infection, as the ubiquitin proteasome- and autophagy lysosome-dependent degradation of I $\kappa$ B $\alpha$  has been reported to be involved in the early and late phases of NF- $\kappa$ B activation, respectively (Ni, 2015). Western blotting revealed a significant increase in pI $\kappa$ B $\alpha$  in hCMEC/D3 cells from 10 to 120 min after *P. gingivalis* infection (Figure 2e and f). Significant decrease in I $\kappa$ B $\alpha$  band was found between 2 and 12 hr after *P. gingivalis* infection (Figure 2g and h), indicating the obvious degradation of I $\kappa$ B $\alpha$  at the late phase of *P. gingivalis* infection.

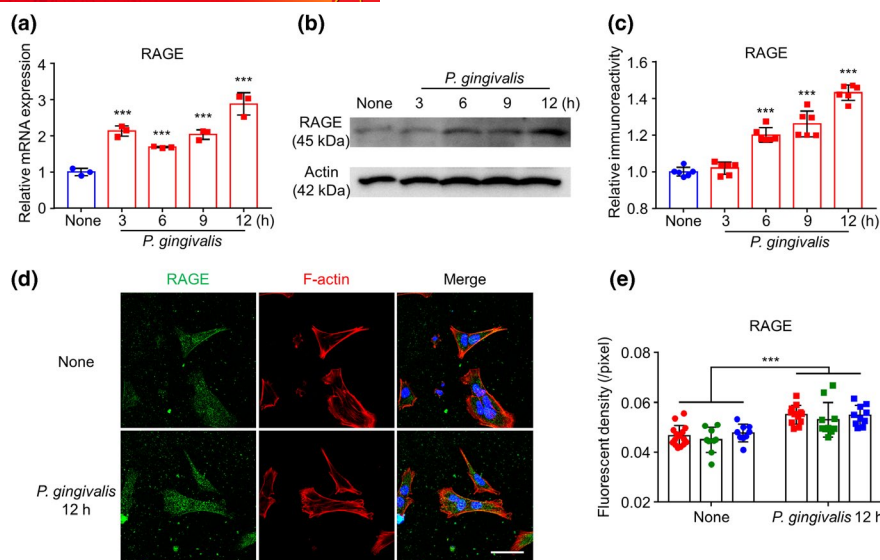


**FIGURE 1** RAGE expression increased in hCMEC/D3 cells after *P. gingivalis* infection. (a) The mean mRNA expression level of RAGE increased in cultured hCMEC/D3 cells after *P. gingivalis* infection ( $n = 3$  independent cell culture preparations, \*\*\* $p < .001$ ; one-way ANOVA). Asterisks indicate a statistically significant difference versus "None" group. (b) The immunoblots show RAGE increased in hCMEC/D3 cells after *P. gingivalis* infection. (c) The quantitative analysis of RAGE in the immunoblots in (b) ( $n = 6$  independent cell culture preparations, \*\*\* $p < .001$ ; one-way ANOVA). Asterisks indicate a statistically significant difference versus "None" group. (d) The immunofluorescent CLMS images of RAGE (green) in hCMEC/D3 cells with Hoechst-stained nuclei (blue) and F-actin (red) 12 hr after *P. gingivalis* infection. Scale bar, 50  $\mu$ m. (e) The quantitative analysis of RAGE fluorescence density in the images in (d) (each color represents one independent cell culture preparations, \*\*\* $p < .01$ ; multiple t-test). Asterisks indicate a statistically significant difference versus "None" group

To further confirm the regulating functions of NF- $\kappa$ B for the RAGE expression in hCMEC/D3 cells after *P. gingivalis* infection, we pre-treated the *P. gingivalis* infected hCMEC/D3 cells with Bay11-7082 (inhibit I $\kappa$ B $\alpha$  phosphorylation) and SN50 (inhibit p65 combining with DNA). Compared to the *P. gingivalis*-infected hCMEC/D3 cells, pretreatment with both Bay11-7082 and SN50 significantly inhibited the *P. gingivalis*-induced increased RAGE expression in hCMEC/D3 cells (Figure 2i). These observations showed that the up-regulated RAGE expression in hCMEC/D3 cells was dependent on the ubiquitin-proteasome degradation of I $\kappa$ B $\alpha$  in the early phase and on the I $\kappa$ B $\alpha$  degradation in the late phase after *P. gingivalis* infection.

### 3.3 | Cathepsin B (CatB) involvement in RAGE up-regulation via NF- $\kappa$ B activation after *P. gingivalis* infection

We next examined the involvement of CatB in the RAGE expression in hCMEC/D3 cells, as we previously found that CatB was involved in the NF- $\kappa$ B activation in phagocytic cells (Ni et al., 2015; Nie et al., 2019). Compared with uninfected cells, the mRNA expression of CatB in hCMEC/D3 cells significantly increased from 3 to 12 hr after *P. gingivalis* infection (Figure 3a), while also the intracellular CatB protein level significantly increased from 3 to 9 hr after *P. gingivalis* infection (Figure 3b and c). The extracellular CatB protein level was also detected from 3 to 12 hr after *P. gingivalis* infection (Figure 3b).

The fact that the CatB increase paralleled the I $\kappa$ B $\alpha$  degradation prompted us to explore the involvement of CatB in I $\kappa$ B $\alpha$  degradation in hCMEC/D3 cells in the late phase after *P. gingivalis* infection. Treatment with the CatB-specific inhibitor CA-074Me partially reversed the *P. gingivalis* infection-induced I $\kappa$ B $\alpha$  degradation at 12 hr after *P. gingivalis* infection (Figure 3d and e). The inhibition of the *P. gingivalis* infection-increased nuclear p65 localization in hCMEC/D3 cells by CA-074Me was further confirmed by immunofluorescent staining (Figure 3f). Furthermore, CA-074Me pretreatment partially inhibited the *P. gingivalis* infection-increased RAGE expression in hCMEC/D3 cells at 12 hr after *P. gingivalis* infection (Figure 3g). These observations indicate that CatB is one of the protease digesting I $\kappa$ B $\alpha$  and partially mediates the RAGE expression in hCMEC/D3 cells after *P. gingivalis* infection.

### 3.4 | RAGE expression mediated A $\beta_{1-42}$ transportation after *P. gingivalis* infection in a transcytosis system

The hCMEC/D3 cell line is typically used for studies of molecule transport from blood-to-brain, including A $\beta$ . To determine the involvement of RAGE in A $\beta$  transportation after *P. gingivalis* infection, we developed a transcytosis system of hCMEC/D3 cells. We cultured hCMEC/D3 cells on transwell inserts, which were then inserted in 24-well plates for 7 days once the endothelial monolayer had formed. To confirm the integrity of the hCMEC/

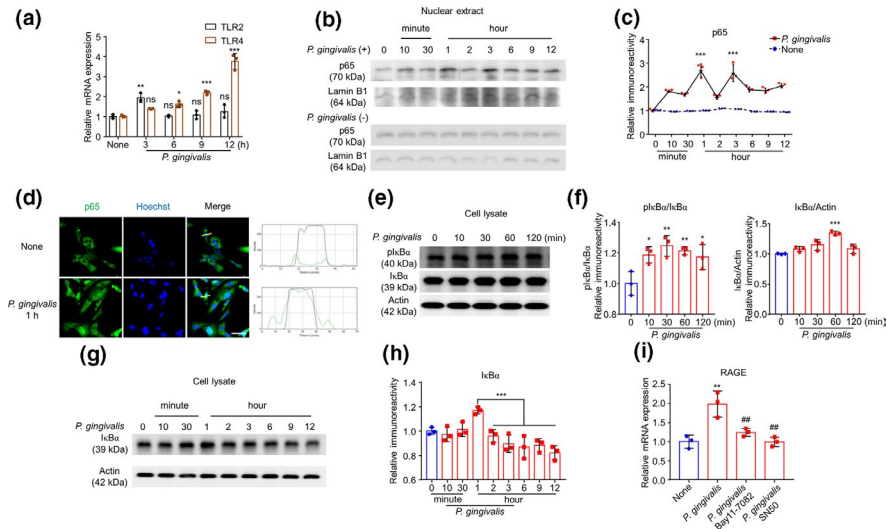


**FIGURE 2** RAGE elevation was dependent on NF- $\kappa$ B activation in hCMEC/D3 cells after *P. gingivalis* infection. (a) The mean mRNA expression level of TLR2/4 in cultured hCMEC/D3 cells after *P. gingivalis* infection ( $n = 3$  independent cell culture preparations, ns: no significant difference,  $*p < .05$ ,  $**p < .01$ ,  $***p < .001$ ; one-way ANOVA). Asterisks indicate a statistically significant difference versus "None" group. (b) The immunoblot images show p65 in nuclear extract with or without *P. gingivalis* infection. (c) The quantitative analysis of p65 in the immunoblots shown in (b) ( $n = 3$  independent cell culture preparations,  $***p < .001$ ; two-way ANOVA). Asterisks indicate a statistically significant difference versus "None" group. (d) The immunofluorescent CLMS images indicating the nuclear translocation of p65 (green) in hCMEC/D3 cells with Hoechst-stained nuclei (blue) after *P. gingivalis* infection for 1 hr. Scale bar, 50  $\mu$ m. (e) The immunoblot images show plkB $\alpha$  and I $\kappa$ B $\alpha$  in cell lysate in hCMEC/D3 cells after *P. gingivalis* infection. (f) The quantitative analysis of immunoblots shown in (e), plkB $\alpha$ /I $\kappa$ B $\alpha$  (left) and I $\kappa$ B $\alpha$ /Actin (right) ( $n = 3$  independent cell culture preparations,  $*p < .05$ ,  $**p < .01$ ,  $***p < .001$ ; one-way ANOVA). Asterisks indicate a statistically significant difference versus "0" group. (g) The immunoblots show I $\kappa$ B $\alpha$  degradation in cell lysate after *P. gingivalis* infection. (h) The quantitative analysis of I $\kappa$ B $\alpha$  in the immunoblots shown in (g) ( $n = 3$  independent cell culture preparations; one-way ANOVA). (i) The effects of Bay11-7082 and SN50, two specific NF- $\kappa$ B inhibitors, on the mRNA expression of RAGE in hCMEC/D3 cells after *P. gingivalis* infection for 12 hr ( $n = 3$  independent cell culture preparations,  $*p < .01$ ,  $##p < .01$ ; one-way ANOVA). Asterisks indicate a statistically significant difference versus "None" group and pounds indicate a statistically significant difference versus "*P. gingivalis*" group

D3 monolayer, we first applied 488-Na-F to the apical side of the transcytosis system. The density of fluorescence in the medium from the basolateral side was determined after 5-min incubation. We detected an obvious fluorescent signal in the no-cell group, which was set as a negative control. Compared with the no-cell group, an 81% reduction in the fluorescent signal was detected in the groups with an hCMEC/D3 monolayer, thus demonstrating the feasibility of the hCMEC/D3 monolayer in the transcytosis system (Figure 4a and b). The transportation of A $\beta_{1-42}$  by the hCMEC/D3 monolayer was then analyzed (Figure 4c). Compared to the uninfected cells, the A $\beta_{1-42}$  fluorescent signal was significantly increased in the medium at the basolateral side of hCMEC/D3 cells after *P. gingivalis* infection. Pre-treatment with the RAGE-specific inhibitor FPS-ZM1 significantly inhibited the fluorescent A $\beta_{1-42}$  (51%) transportation from the apical side to the basolateral side in the *P. gingivalis*-infected hCMEC/D3 cells at 12 hr after *P. gingivalis* infection (Figure 4d). It was noted that neither *P. gingivalis* nor FPS-ZM1 affected the integrity of the hCMEC/D3 monolayer, as no significant increase in 488-Na-F was detected in the basolateral medium (Figure 4b). These observations suggest that A $\beta_{1-42}$  transportation via hCMEC/D3 cells was induced by *P. gingivalis* infection, and the increased expression of RAGE was responsible for A $\beta_{1-42}$  transportation during *P. gingivalis* infection.

### 3.5 | Increased RAGE expression in cerebral endothelial cells and the induction of A $\beta_{1-42}$ around cerebral endothelial cells in mice after systemic *P. gingivalis* infection

To determine the RAGE expression is increased in the cerebral endothelial cell which is related to A $\beta$  influx into brain in vivo, we finally examined the RAGE expression on cerebral endothelial cells in mouse brains after systemic *P. gingivalis* infection. The timing of systemic *P. gingivalis* infection is shown as an illustration (Figure 5a). The expression level of CatB and RAGE, as well as the localization of p65 and A $\beta_{1-42}$  in cerebral endothelial cells were determined by immunofluorescent staining. Compared to the saline-treated mice, the CatB expression in CD31-positive cerebral endothelial cells was significantly increased (Figure 5b and d). The co-localization between p65 and Hoechst was significantly increased, which means more NF- $\kappa$ B activation in cerebral endothelial cells after systemic *P. gingivalis* infection (Figure 5c and e). Additionally, RAGE expression in CD31-positive cerebral endothelial cells was significantly increased (1.8-fold), and the co-localization between RAGE and CD31 was significantly increased (2.7-fold) in the mouse brain after 3 weeks of systemic *P. gingivalis* infection (Figure 6a, c and d). Furthermore, compared to the scarce A $\beta_{1-42}$  signal in the brain of saline-treated



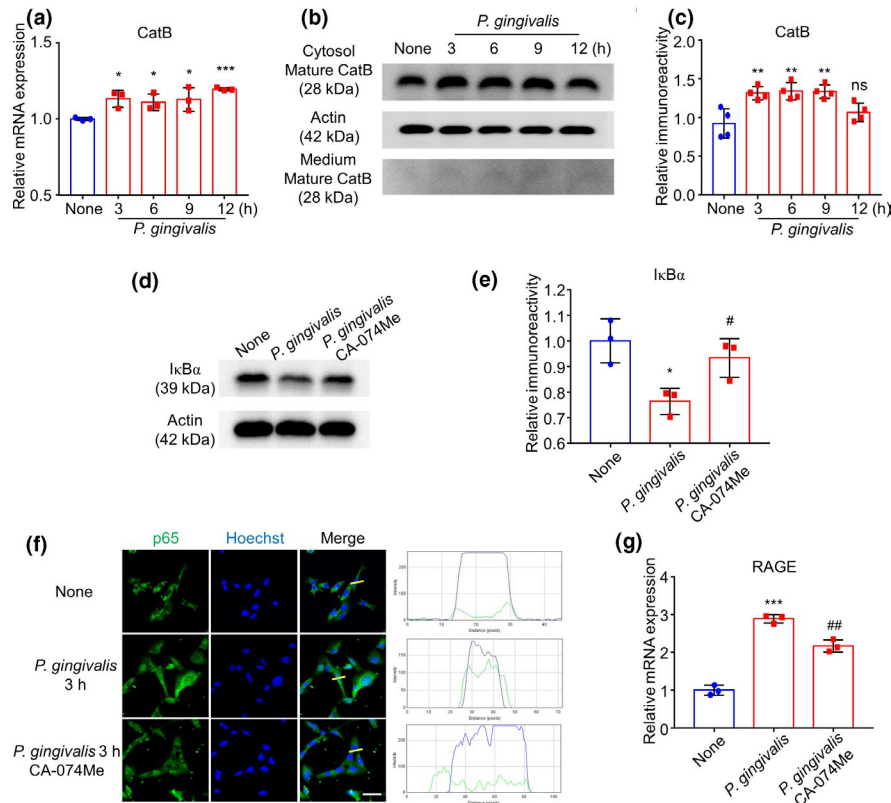


**FIGURE 3** CatB/NF- $\kappa$ B pathway regulated late-phase expression of RAGE after *P. gingivalis* infection. (a) The mean mRNA expression level of CatB of cultured hCMEC/D3 cells increased after *P. gingivalis* infection ( $n = 3$  independent cell culture preparations,  $*p < .05$ ,  $***p < .001$ ; one-way ANOVA). Asterisks indicate a statistically significant difference versus "None" group. (b) The immunoblots show mature CatB in cytosol and medium in hCMEC/D3 after *P. gingivalis* infection. (c) The quantitative analysis of cytosol CatB in (b) ( $n = 4$  independent cell culture preparations, ns: no significant difference,  $**p < .01$ ; one-way ANOVA). Asterisks indicate a statistically significant difference versus "None" group. (d) The effect of CA-074Me, a specific CatB inhibitor, on I $\kappa$ B $\alpha$  degradation after *P. gingivalis* infection for 12 hr. (e) The quantitative analysis of (d) ( $n = 3$  independent cell culture preparations,  $*p < .05$ ,  $\#p < .05$ ; one-way ANOVA). Asterisks indicate a statistically significant difference versus "None" group and pounds indicate a statistically significant difference versus "*P. gingivalis*" group. (f) The effect of CA-074Me on the nuclear translocation of p65 (green) in hCMEC/D3 cells with Hoechst-stained nuclei (blue) at 3 hr after *P. gingivalis* infection. Scale bar, 50  $\mu$ m. (g) The effect of CA-074Me on the mRNA expression of RAGE in hCMEC/D3 cells after *P. gingivalis* infection ( $n = 3$  independent cell culture preparations,  $***p < .001$ ,  $##p < .01$ ; one-way ANOVA). Asterisks indicate a statistically significant difference versus "None" group and pounds indicate a statistically significant difference versus "*P. gingivalis*" group

mice, the A $\beta_{1-42}$  signal in the brain parenchyma localized around the CD31-positive cerebral endothelial cells was significantly increased (6.8-fold) in mice after systemic *P. gingivalis* infection (Figure 6b and e). In addition, the expression of RAGE on cerebral endothelial cells was positively correlated with that of A $\beta_{1-42}$  in the systemic *P. gingivalis* infected mice ( $r = 0.6205$ , Figure 6f). Furthermore, significant memory decline was found at week 3 of the mice with *P. gingivalis* infection in comparison to that in saline-treated mice (Figure 6g). These observations showed that the induced A $\beta_{1-42}$  in the brain parenchyma was close to the significantly increased level of RAGE-brain endothelial cells that were expressed in middle-aged mice after chronic systemic *P. gingivalis* infection.

## 4 | DISCUSSION

The major finding of this study was our determination that the CatB/NF- $\kappa$ B-dependent RAGE expression mediates the A $\beta$  influx after

*P. gingivalis* infection using an in vitro model of the BBB and middle-aged mice (Summarized in Figure 7). We thus demonstrated a new mechanism underlying the influence of systemic periodontal bacterial infection on the initiation and pathological progression of AD.

Structurally as a transmembrane receptor, RAGE is expressed in multiple types of cells, including cerebral endothelial cells (Derk, MacLean, Juranek, & Schmidt, 2018). *P. gingivalis* increased the RAGE expression in hCMEC/D3 cells, which is consistent with the previous study that brain endothelial RAGE expression was increased in AD mouse models and AD patients (Miller et al., 2008). *P. gingivalis* has been reported to activate TLR2/4/MyD88/NF- $\kappa$ B pathway in macrophage (Papadopoulos et al., 2013). In this study, we found that the mRNA level of both TLR2 and TLR4 were increased at early and late phase, respectively, suggesting that TLR2 and TLR4 cooperatively responded to the *P. gingivalis* in hCMEC/D3 cells. It is commonly accepted that TLR2 and TLR4 could lead to a signaling cascade that ultimately resulted in the activation of NF- $\kappa$ B. In this study, we also detected the activation of NF- $\kappa$ B in hCMEC/D3

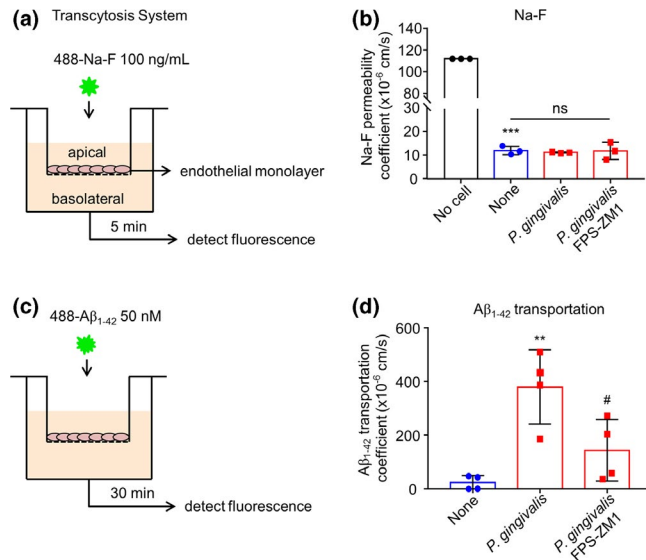


**FIGURE 4** RAGE expression mediated A $\beta_{1-42}$  transportation after *P. gingivalis* infection in a transcytosis system. (a) The schematic of the in vitro transcytosis system for Na-F transportation. (b) The quantitative analysis of Na-F (100 ng/mL) permeability after *P. gingivalis* infection for 12 hr in the presence or absence of FPS-ZM1 pre-treatment. The “No cell” means no cell in the transcytosis system ( $n = 3$  independent cell culture preparations, ns: no significant difference, \*\*\* $p < .001$ ; one-way ANOVA). Asterisks indicate a statistically significant difference versus “No cell” group and “ns” indicates the result compared with “None” group. (c) The schematic of the in vitro transcytosis system for A $\beta_{1-42}$  transportation. (d) The transportation of A $\beta_{1-42}$  from apical to basolateral compartment after *P. gingivalis* infection for 12 hr. ( $n = 4$  independent cell culture preparations, \*\* $p < .01$ , #  $p < .05$ , one-way ANOVA). Asterisks indicate a statistically significant difference compared with “None” group and pounds indicate a statistically significant difference compared with “*P. gingivalis*” group

cells after *P. gingivalis* treatment. However, the activation of NF- $\kappa$ B showed two peaks revealing by the nuclear translocation of p65 at 1 and 3 hr after *P. gingivalis* treatment. To further study the activation status of NF- $\kappa$ B, we separately examined the I $\kappa$ B $\alpha$  phosphorylation/proteasome degradation system and I $\kappa$ B $\alpha$ /CatB degradation system. We found *P. gingivalis* induced I $\kappa$ B $\alpha$  phosphorylation/proteasome-dependent activation of NF- $\kappa$ B at early phase, while induced CatB-dependent activation of NF- $\kappa$ B at late phase in hCMEC/D3 cells. RAGE promoter possesses three NF- $\kappa$ B-binding sites, the increased RAGE mRNA may be because of the two times activation of NF- $\kappa$ B (Li, 1997). It was noted that *P. gingivalis* induced NF- $\kappa$ B activation and CatB production may be synergized because CatB promoter also possessed NF- $\kappa$ B-binding sites (Bien et al., 2004).

The RAGE expression in cerebral endothelial cells plays an important role in facilitating the influx of circulating A $\beta$  into the brain across the BBB (Deane et al., 2003; Schmidt, Yan, Yan, & Stern, 2001). In this study, an increase in the A $\beta_{1-42}$  transportation across the *P. gingivalis*-infected hCMEC/D3 cells compared to the uninfected cells was noted, strongly suggesting that the A $\beta_{1-42}$  influx was dramatically up-regulated after *P. gingivalis* infection (Figure 4).

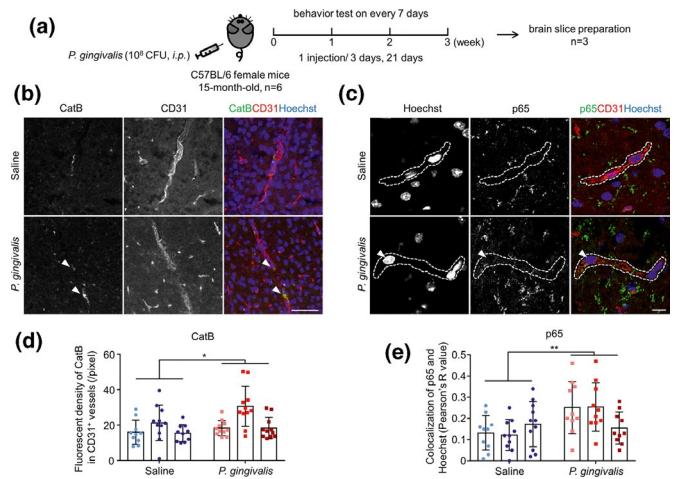


**FIGURE 5** Increased CatB and translocation of p65 in cerebral endothelial cells of mice after systemic *P. gingivalis* infection. (a) Time schedule of systemic *P. gingivalis* infection and behavior test. (b) The immunofluorescent CLMS images of brain slice stained with CatB (green), CD31 (red), and Hoechst (blue) after systemic *P. gingivalis* infection. (c) The immunofluorescent CLMS images of brain slice stained with p65 (green), CD31 (red), and Hoechst (blue) after systemic *P. gingivalis* infection. Dash lines marked the location of blood vessels. (d) The quantitative analysis of CatB fluorescence density in CD31 $^{+}$  vessels in the images in (b). (e) Co-localization analysis of p65 and Hoechst in the images in (c) using ImageJ (COLOC 2 plugin of Fiji is just ImageJ). Three mice per group were used and each mouse has its own color. Asterisks indicate a statistically significant difference versus “Saline” group using multiple t-test. \* $p < .05$ , \*\* $p < .01$ . Scale bars in b: 50  $\mu$ m; c: 10  $\mu$ m

In our in vitro transcytosis system, the Na-F permeability across the monolayer of hCMEC/D3 cells were not reduced by *P. gingivalis* infection at MOI = 5 for 12 hr, confirming that the *P. gingivalis* infection-induced A $\beta_{1-42}$  influx via hCMEC/D3 cells was mediated by the “transport barrier” without disrupting the “physical barrier” (cell monolayer) (Poggesi, Pasi, Pescini, Pantoni, & Inzitari, 2016). The *P. gingivalis* infection-induced A $\beta_{1-42}$  influx was markedly reduced by pre-treatment with FPS-ZM1, a specific inhibitor of RAGE, providing the first evidence that the RAGE expression in cerebral endothelial cells mediates the A $\beta$  influx after *P. gingivalis* infection. Of note, the *P. gingivalis* infection-induced mild increase in the RAGE expression in the cerebral endothelial cells was related to a dramatic A $\beta$  influx in the present in vitro A $\beta$  transportation system, strongly indicating that the increased RAGE expression in the cerebral endothelial cells efficiently affected the A $\beta$  influx during *P. gingivalis* infection.

The present in vitro observations were further supported by the parallel increase in the RAGE expression in cerebral endothelial cells and the A $\beta$  loads in the brain parenchyma around the cerebral vasculature in middle-aged mice with a significant memory decline after 3 weeks of chronic systemic *P. gingivalis* infection. The increased expression level of CatB in cerebral endothelial cells was also found in *P. gingivalis* infected mice. To our knowledge, this is the first evidence of cerebrovascular-related amyloid genesis induced by systemic *P. gingivalis* infection, highlighting a new mechanism underlying the effect of periodontitis on AD pathologies,

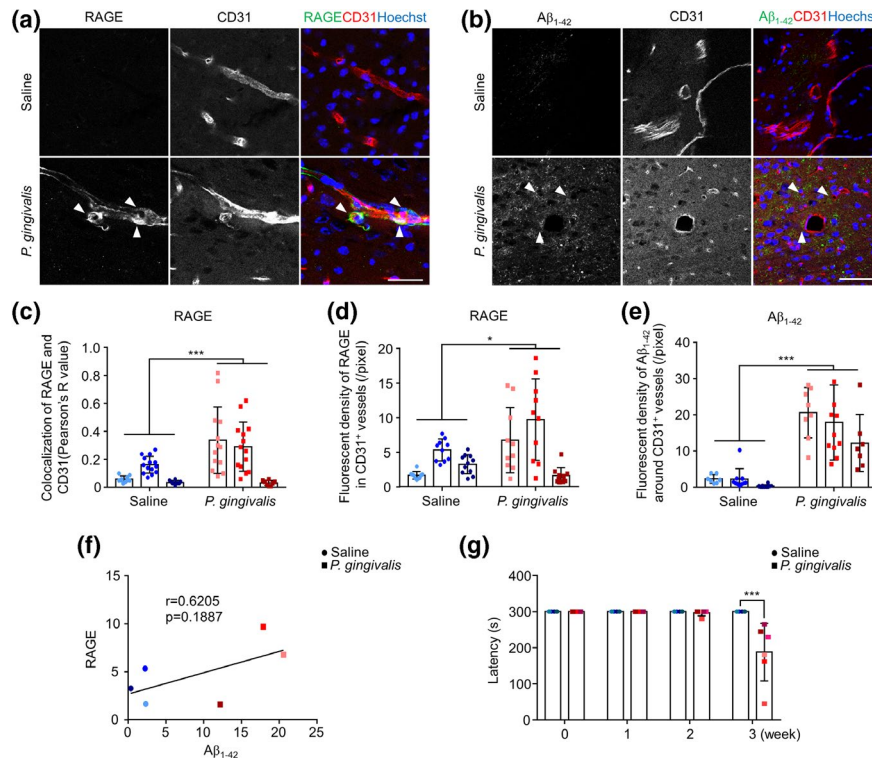


**FIGURE 6** Increased RAGE expression in cerebral endothelial cells and the induction of Aβ<sub>1-42</sub> around cerebral endothelial cells of mice after systemic *P. gingivalis* infection. (a) The immunofluorescent CLMS images of brain slice stained with RAGE (green), CD31 (red), and Hoechst (blue) after systemic *P. gingivalis* infection. (b) The immunofluorescent CLMS images of brain slice stained with Aβ<sub>1-42</sub> (green), CD31 (red), and Hoechst (blue) after systemic *P. gingivalis* infection. (c) Co-localization analysis of RAGE and CD31 in the images in (a) using COLOC 2 plugin. (d) The quantitative analysis of RAGE fluorescence density in CD31<sup>+</sup> vessels in the images in (a). (e) The quantitative analysis of Aβ<sub>1-42</sub> fluorescence density around CD31<sup>+</sup> vessels in the images in (b). (f) Pearson's correlation between the fluorescence density of RAGE and Aβ<sub>1-42</sub>. (a-f) Three mice per group were used and each mouse has its own color. (g) Memory decline in mice after 3 weeks of systemic *P. gingivalis* infection ( $n = 6$  mice/group). Asterisks indicate a statistically significant difference versus "Saline" group using multiple *t*-test. \* $p < .05$ , \*\* $p < .01$ , \*\*\* $p < .001$ . Scale bar, 50 μm

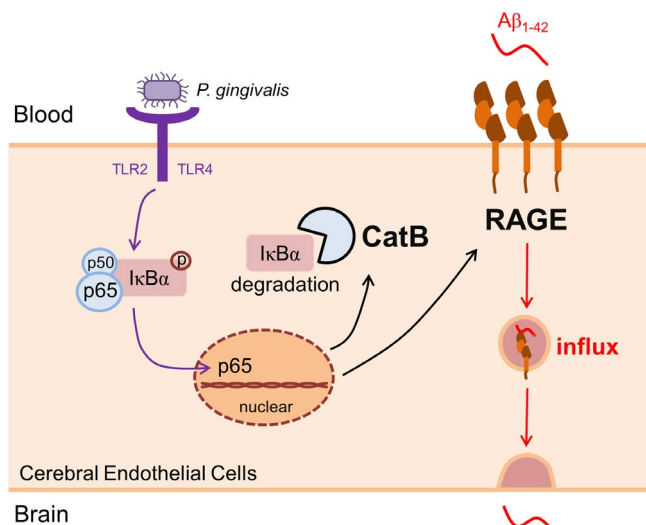


**FIGURE 7** The schematic of the critical role of RAGE in cerebral endothelial cell after *P. gingivalis* infection. *P. gingivalis* activates NF-κB pathway through binding TLR2/4, triggers transcription of RAGE and CatB. The increased CatB further involves in RAGE up-regulation via regulating NF-κB activation. At last, elevated RAGE mediates the influx of Aβ from blood to the brain

as cerebrovascular-related amyloidogenesis has been found in over 80% of AD patients (Attems & Jellinger, 2014; Jellinger & Attems, 2005) and this condition positively correlates with a cognitive decline (Thal, Griffin, de Vos, & Ghebremedhin, 2008; Weller, Boche, & Nicoll, 2009). The finding that systemic *P. gingivalis* infection induced the cerebral RAGE expression/cerebrovascular amyloidogenesis in middle-aged mice is significant because around 70% of periodontitis morbidity has been found in middle-aged individuals (Eke et al., 2012, 2015) and the RAGE up-regulation with continues up until middle age (Osgood, Miller, Messier, Gonzalez, & Silverberg, 2017). In combination with our recent findings that the peripheral pools of Aβ are increased during *P. gingivalis* infection (Nie et al., 2019), the synergic interplay between the cerebral RAGE expression and peripheral Aβ generation contributes to the cerebral amyloidogenesis during chronic *P. gingivalis* infection, as the circulating Aβ can be transferred into the brain (Deane & Zlokovic, 2007), thereby increasing the Aβ levels in the brains of AD patients (Donahue et al., 2006). Given the contribution of RAGE up-regulation and Aβ/RAGE interaction to AD pathogenesis (Donahue et al., 2006; Jaynes & Provias, 2008; Kook et al., 2012), an elevated cerebral RAGE expression may be a new therapeutic strategy for AD (Zlokovic, 2008). We are currently investigating the

influence of *P. gingivalis*/LPS on other outcomes of the cerebral microenvironment in a separate study.

Periodontal disease positive association with AD was thought to be induced by systemic inflammation (Gaur & Agnihotri, 2015). Chronic periodontitis induced increased pro-inflammatory cytokines in periphery tissues and the circulating system decreased BBB integrity, and activated microglia. Therefore, chronic periodontitis and infection with *P. gingivalis* have been identified as a significant risk factor for developing A $\beta$  plaque, dementia, and AD (Dominy et al., 2019). Beside of this indirect relationship between periodontal disease and AD, we found *P. gingivalis* induced increased A $\beta$  influx directly through RAGE in brain endothelial cells. Therefore, it will be interesting to study the positive association between periodontitis, RAGE expression in brain endothelial cell, and brain A $\beta$  accumulation in patients with AD.

In this study, the *P. gingivalis*-induced I $\kappa$ B $\alpha$  degradation was partially reduced by the CatB-specific inhibitor in hCMEC/D3 cells, indicating that CatB participates in chronic NF- $\kappa$ B activation in cerebral endothelial cells after *P. gingivalis* infection. The present finding was supported by the previous report that CatB is involved in NF- $\kappa$ B activation by lysosome degradation in microglia, the primary immune cells in the brain (Ni et al., 2015). This, along with our previous findings of the involvements of CatB in A $\beta$  generation in neurons of the brain as well as in peripheral inflammatory monocytes/macrophages after *P. gingivalis* infection/exposure to *P. gingivalis* LPS (Nie et al., 2019; Wu et al., 2017), suggests that CatB may involve in the pathogenesis of AD for prolonging NF- $\kappa$ B activation with its enzymatic functions during *P. gingivalis* infection. Of note, increased CatB in the hCMEC/D3 cells (human cerebral endothelial cells) was induced by *P. gingivalis* infection at MOI = 5, while the expression of CatB in human umbilical vein endothelial cells (endothelial cells of peripheral blood vessels) had no change after *P. gingivalis* infection at MOI = 200 (Huck, Elkaim, Davideau, & Tenenbaum, 2012), suggesting different endothelial cells have different responses to *P. gingivalis* infection. The sensitive response to microbial infection of cerebral endothelial cells may contribute to the CatB/NF- $\kappa$ B/RAGE-dependent A $\beta$  influx.

In conclusion, this study demonstrated that the CatB/NF- $\kappa$ B activation-dependent RAGE up-regulation in cerebral endothelial cells mediates cerebrovascular-related amyloidogenesis during *P. gingivalis* infection, highlighting a new mechanism for the involvement of periodontitis in AD and pathological process.

## ACKNOWLEDGMENTS

This work is supported by the Japanese KAKENHI Grant Number 16K11478 (Grants-in-Aid for Scientific Research to Z.W.), Grant Number JP17K17093 (a Grant-in-Aid for Young Scientists to J.N.), and the research grant for OBT research center from the Kyushu University (to Z.W.).

All experiments were conducted in compliance with the ARRIVE guidelines.

## CONFLICT OF INTEREST

The authors F. Zeng, J. Ni, Y. Liu, W. Huang, H. Qing, T. Kadowaki, H. Kashiwazaki, and Z. Wu declare that they have no conflict of interest.

## OPEN RESEARCH BADGES



This article has received a badge for \*Open Materials\* because it provided all relevant information to reproduce the study in the manuscript. More information about the Open Science badges can be found at <https://cos.io/our-services/open-science-badges/>.

## ORCID

Fan Zeng <https://orcid.org/0000-0002-4016-7302>

Hong Qing <https://orcid.org/0000-0003-2820-450X>

Junjun Ni <https://orcid.org/0000-0001-8486-8146>

Zhou Wu <https://orcid.org/0000-0002-4910-9037>

## REFERENCES

- Abbott, N. J., Ronnback, L., & Hansson, E. (2006). Astrocyte-endothelial interactions at the blood-brain barrier. *Nature Reviews Neuroscience*, 7, 41–53. <https://doi.org/10.1038/nrn1824>
- Attems, J., & Jellinger, K. A. (2014). The overlap between vascular disease and Alzheimer's disease-lessons from pathology. *BMC Medicine*, 12, 206. <https://doi.org/10.1186/s12916-014-0206-2>
- Bielecka, E., Scavenius, C., Kantyka, T., Jusko, M., Mizgalska, D., Szmigielski, B., ... Potempa, J. (2014). Peptidyl arginine deiminase from *Porphyromonas gingivalis* abolishes anaphylatoxin C5a activity. *Journal of Biological Chemistry*, 289, 32481–32487.
- Bien, S., Ritter, C. A., Gratz, M., Sperker, B., Sonnemann, J., Beck, J. F., & Kroemer, H. K. (2004). Nuclear factor-kappaB mediates up-regulation of cathepsin B by doxorubicin in tumor cells. *Molecular Pharmacology*, 65, 1092–1102.
- Bu, X. L., Xiang, Y., Jin, W. S., Wang, J., Shen, L.-L., Huang, Z.-L., ... Wang, Y.-J. (2018). Blood-derived amyloid-beta protein induces Alzheimer's disease pathologies. *Molecular Psychiatry*, 23, 1948–1956.
- Charan, J., & Kantharia, N. D. (2013). How to calculate sample size in animal studies? *Journal of Pharmacology and Pharmacotherapeutics*, 4, 303–306. <https://doi.org/10.4103/0976-500X.119726>
- Chen, C. D., Zeldich, E., Khodr, C., Camara, K., Tung, T. Y., Lauder, E. C., ... Abraham, C. R. (2019). Small molecule amyloid-beta protein precursor processing modulators lower amyloid-beta peptide levels via cKit signaling. *Journal of Alzheimer's Disease*, 67, 1089–1106.
- Deane, R., Du Yan, S., Subramanyam, R. K., LaRue, B., Jovanovic, S., Hogg, E., ... Zlokovic, B. (2003). RAGE mediates amyloid  $\beta$  peptide transport across the blood-brain barrier and accumulation in brain. *Nature Medicine*, 9, 907. <https://doi.org/10.1038/nm890>
- Deane, R., & Zlokovic, B. V. (2007). Role of the blood-brain barrier in the pathogenesis of Alzheimer's disease. *Current Alzheimer Research*, 4, 191–197.
- Derk, J., MacLean, M., Juranek, J., & Schmidt, A. M. (2018). The receptor for advanced glycation endproducts (RAGE) and mediation of inflammatory neurodegeneration. *Journal of Alzheimer's Disease & Parkinsonism*, 8(1), 421. <https://doi.org/10.4172/2161-0460.1000421>
- Di Marco, A., Gonzalez Paz, O., Fini, I., Vignone, D., Cellucci, A., Battista, M. R., ... Muñoz-Sanjuán, I. (2019). Application of an in vitro blood-brain barrier model in the selection of experimental drug candidates for the treatment of huntington's disease. *Molecular Pharmaceutics*,





- 16, 2069–2082. <https://doi.org/10.1021/acs.molpharmac.9b00042>
- Dominy, S. S., Lynch, C., Ermini, F., Malgorzata, B., Marczyk, A., Konradi, A., ... Potempa, J. (2019). Porphyromonas gingivalis in Alzheimer's disease brains: Evidence for disease causation and treatment with small-molecule inhibitors. *Science Advances*, 5, eaau3333.
- Donahue, J. E., Flaherty, S. L., Johanson, C. E., Duncan, J. A., Silverberg, G. D., Miller, M. C., ... Stopa, E. G. (2006). RAGE, LRP-1, and amyloid-beta protein in Alzheimer's disease. *Acta Neuropathologica*, 112, 405–415. <https://doi.org/10.1007/s00401-006-0115-3>
- Eke, P. I., Dye, B. A., Wei, L., Slade, G. D., Thornton-Evans, G. O., Borgnakke, W. S., ... Genco, R. J. (2015). Update on prevalence of periodontitis in adults in the United States: NHANES 2009 to 2012. *Journal of Periodontology*, 86, 611–622. <https://doi.org/10.1902/jop.2015.140520>
- Eke, P. I., Dye, B. A., Wei, L., Thornton-Evans, G. O., Genco, R. J., Surveillance, C. P. D., & workgroup: James Beck, G. D. R. P., (2012). Prevalence of periodontitis in adults in the United States: 2009 and 2010. *Journal of Dental Research*, 91, 914–920. <https://doi.org/10.1177/0022034512457373>
- Evin, G., Zhu, A., Holsinger, R. M. D., Masters, C. L., & Li, Q.-X. (2003). Proteolytic processing of the Alzheimer's disease amyloid precursor protein in brain and platelets. *Journal of Neuroscience Research*, 74, 386–392. <https://doi.org/10.1002/jnr.10745>
- Gaur, S., & Agnihotri, R. (2015). Alzheimer's disease and chronic periodontitis: Is there an association? *Geriatr Gerontol Int*, 15, 391–404. <https://doi.org/10.1111/ggi.12425>
- Hodson, R. (2018). Alzheimer's disease. *Nature*, 559, S1. <https://doi.org/10.1038/d41586-018-05717-6>
- Huck, O., Elkaim, R., Davideau, J. L., & Tenenbaum, H. (2012). Porphyromonas gingivalis and its lipopolysaccharide differentially regulate the expression of cathepsin B in endothelial cells. *Mol. Oral Microbiol.*, 27, 137–148. <https://doi.org/10.1111/j.2041-1014.2012.00638.x>
- Iadecola, C. (2013). The pathobiology of vascular dementia. *Neuron*, 80, 844–866. <https://doi.org/10.1016/j.neuron.2013.10.008>
- Ide, M., Harris, M., Stevens, A., Sussams, R., Hopkins, V., Culliford, D., ... Holmes, C. (2016). Periodontitis and cognitive decline in Alzheimer's disease. *PLoS One*, 11, e0151081. <https://doi.org/10.1371/journal.pone.0151081>
- Ilievski, V., Zuchowska, P. K., Green, S. J., Toth, P. T., Ragozzino, M. E., Le, K., ... Watanabe, K. (2018). Chronic oral application of a periodontal pathogen results in brain inflammation, neurodegeneration and amyloid beta production in wild type mice. *PLoS One*, 13, e0204941. <https://doi.org/10.1371/journal.pone.0204941>
- Jellinger, K. A., & Attems, J. (2005). Prevalence and pathogenic role of cerebrovascular lesions in Alzheimer disease. *Journal of the Neurological Sciences*, 229–230, 37–41. <https://doi.org/10.1016/j.jns.2004.11.018>
- Jeynes, B., & Provias, J. (2008). Evidence for altered LRP/RAGE expression in Alzheimer lesion pathogenesis. *Current Alzheimer Research*, 5, 432–437.
- Kook, S. Y., Hong, H. S., Moon, M., Ha, C. M., Chang, S., & Mook-Jung, I. (2012). Abeta1(–)4(2)-RAGE interaction disrupts tight junctions of the blood-brain barrier via Ca2(+)-calcineurin signaling. *Journal of Neuroscience*, 32, 8845–8854.
- Kovari, E., Herrmann, F. R., Hof, P. R., & Bouras, C. (2013). The relationship between cerebral amyloid angiopathy and cortical microinfarcts in brain ageing and Alzheimer's disease. *Neuropathology and Applied Neurobiology*, 39, 498–509. <https://doi.org/10.1111/nan.12003>
- Kuo, Y. M., Kokjohn, T. A., Watson, M. D., Woods, A. S., Cotter, R. J., Sue, L. I., ... Roher, A. E. (2000). Elevated abeta42 in skeletal muscle of Alzheimer disease patients suggests peripheral alterations of AbetaPP metabolism. *American Journal of Pathology*, 156, 797–805.
- Li, J., & Schmidt, A. M. (1997). Characterization and functional analysis of the promoter of RAGE, the receptor for advanced glycation end products. *Journal of Biological Chemistry*, 272, 16498–16506. <https://doi.org/10.1074/jbc.272.26.16498>
- Liu, Y., Wu, Z., Nakanishi, Y., Ni, J., Hayashi, Y., Takayama, F., ... Nakanishi, H. (2017). Infection of microglia with Porphyromonas gingivalis promotes cell migration and an inflammatory response through the gingipain-mediated activation of protease-activated receptor-2 in mice. *Scientific Reports*, 7, 11759. <https://doi.org/10.1038/s41598-017-12173-1>
- Luo, C., Zhang, Y.-L., Luo, W., Zhou, F. H., Li, C.-Q., Xu, J.-M., & Dai, R.-P. (2015). Differential effects of general anesthetics on anxiety-like behavior in formalin-induced pain: Involvement of ERK activation in the anterior cingulate cortex. *Psychopharmacology (Berl)*, 232, 4433–4444. <https://doi.org/10.1007/s00213-015-4071-2>
- Miller, M. C., Tavares, R., Johanson, C. E., Hovanesian, V., Donahue, J. E., Gonzalez, L., ... Stopa, E. G. (2008). Hippocampal RAGE immunoreactivity in early and advanced Alzheimer's disease. *Brain Research*, 1230, 273–280. <https://doi.org/10.1016/j.brainres.2008.06.124>
- Ni, J., Wu, Z., Peterts, C., Yamamoto, K., Qing, H., & Nakanishi, H. (2015). The critical role of Proteolytic relay through cathepsins B and E in the phenotypic change of microglia/macrophage. *Journal of Neuroscience*, 35, 12488–12501. <https://doi.org/10.1523/JNEUROSCI.1599-15.2015>
- Nie, R., Wu, Z., Ni, J., Zeng, F., Yu, W., Zhang, Y., & Zhou, Y. (2019). Porphyromonas gingivalis infection induces amyloid-beta accumulation in monocytes/macrophages. *Journal of Alzheimer's Disease*, 72, 479–494.
- Noble, J. M., Borrell, L. N., Papapanou, P. N., Elkind, M. S. V., Scarmeas, N., & Wright, C. B. (2009). Periodontitis is associated with cognitive impairment among older adults: Analysis of NHANES-III. *Journal of Neurology, Neurosurgery and Psychiatry*, 80, 1206–1211.
- Osgood, D., Miller, M. C., Messier, A. A., Gonzalez, L., & Silverberg, G. D. (2017). Aging alters mRNA expression of amyloid transporter genes at the blood-brain barrier. *Neurobiology of Aging*, 57, 178–185. <https://doi.org/10.1016/j.neurobiolaging.2017.05.011>
- Papadopoulos, G., Shaik-Dasthagirisahab, Y. B., Huang, N., Viglianti, G. A., Henderson, A. J., Kantarci, A., & Gibson, F. C. III (2017). Immunologic environment influences macrophage response to Porphyromonas gingivalis. *Molecular Oral Microbiology*, 32, 250–261.
- Papadopoulos, G., Weinberg, E. O., Massari, P., Gibson, F. C., Wetzler, L. M., Morgan, E. F., & Genco, C. A. (2013). Macrophage-specific TLR2 signaling mediates pathogen-induced TNF-dependent inflammatory oral bone loss. *The Journal of Immunology*, 190, 1148–1157. <https://doi.org/10.4049/jimmunol.1202511>
- Poggesi, A., Pasi, M., Pescini, F., Pantoni, L., & Inzitari, D. (2016). Circulating biologic markers of endothelial dysfunction in cerebral small vessel disease: A review. *Journal of Cerebral Blood Flow and Metabolism*, 36, 72–94. <https://doi.org/10.1038/jcbfm.2015.116>
- Poole, S., Singhrao, S. K., Kesavalu, L., Curtis, M. A., & Crean, S. (2013). Determining the presence of periodontopathic virulence factors in short-term postmortem Alzheimer's disease brain tissue. *Journal of Alzheimer's Disease*, 36, 665–677. <https://doi.org/10.3233/JAD-121918>
- Reife, R. A., Coats, S. R., Al-Qutub, M., Dixon, D. M., Braham, P. A., Billharz, R. J., ... Darveau, R. P. (2006). Porphyromonas gingivalis lipopolysaccharide lipid A heterogeneity: Differential activities of tetra- and penta-acylated lipid A structures on E-selectin expression and TLR4 recognition. *Cellular Microbiology*, 8, 857–868. <https://doi.org/10.1111/j.1462-5822.2005.00672.x>
- Roher, A. E., & Kokjohn, T. A. (2009). Commentary on "Alzheimer's disease drug development and the problem of the blood-brain barrier." Alzheimer's disease drugs: More than one barrier to breach. *Alzheimer's & Dementia: the Journal of the Alzheimer's Association*, 5, 437–438.



- Sagare, A. P., Deane, R., & Zlokovic, B. V. (2012). Low-density lipoprotein receptor-related protein 1: A physiological A $\beta$  homeostatic mechanism with multiple therapeutic opportunities. *Pharmacology & Therapeutics*, 136, 94–105. <https://doi.org/10.1016/j.pharmthera.2012.07.008>
- Schmidt, A. M., Yan, S. D., Yan, S. F., & Stern, D. M. (2001). The multiligand receptor RAGE as a progression factor amplifying immune and inflammatory responses. *Journal of Clinical Investigation*, 108, 949–955. <https://doi.org/10.1172/JCI200114002>
- Slaney, J. M., Gallagher, A., Aduse-Opoku, J., Pell, K., & Curtis, M. A. (2006). Mechanisms of resistance of *Porphyromonas gingivalis* to killing by serum complement. *Infection and Immunity*, 74, 5352–5361. <https://doi.org/10.1128/IAI.00304-06>
- Sparks Stein, P., Steffen, M. J., Smith, C., Jicha, G., Ebersole, J. L., Abner, E., & Dawson, D. (2012). Serum antibodies to periodontal pathogens are a risk factor for Alzheimer's disease. *Alzheimer's & Dementia: the Journal of the Alzheimer's Association*, 8, 196–203. <https://doi.org/10.1016/j.jalz.2011.04.006>
- Thal, D. R., Griffin, W. S., de Vos, R. A., & Ghebremedhin, E. (2008). Cerebral amyloid angiopathy and its relationship to Alzheimer's disease. *Acta Neuropathologica*, 115, 599–609. <https://doi.org/10.1007/s00401-008-0366-2>
- Weller, R. O., Boche, D., & Nicoll, J. A. (2009). Microvasculature changes and cerebral amyloid angiopathy in Alzheimer's disease and their potential impact on therapy. *Acta Neuropathologica*, 118, 87–102. <https://doi.org/10.1007/s00401-009-0498-z>
- Wu, Z., Ni, J., Liu, Y., Teeling, J. L., Takayama, F., Collcutt, A., ... Nakanishi, H. (2017). Cathepsin B plays a critical role in inducing Alzheimer's disease-like phenotypes following chronic systemic exposure to lipopolysaccharide from *Porphyromonas gingivalis* in mice. *Brain, Behavior, and Immunity*, 65, 350–361. <https://doi.org/10.1016/j.bbi.2017.06.002>
- Yan, S. D., Chen, X. I., Fu, J., Chen, M., Zhu, H., Roher, A., ... Schmidt, A. M. (1996). RAGE and amyloid  $\beta$  peptide neurotoxicity in Alzheimer's disease. *Nature*, 382, 685. <https://doi.org/10.1038/382685a0>
- Zlokovic, B. V. (2008). New therapeutic targets in the neurovascular pathway in Alzheimer's disease. *Neurotherapeutics: the Journal of the American Society for Experimental Neurotherapeutics*, 5, 409–414. <https://doi.org/10.1016/j.nurt.2008.05.011>

**How to cite this article:** ZengF, Liu Y, Huang W, et al.

Receptor for advanced glycation end products up-regulation in cerebral endothelial cells mediates cerebrovascular-related amyloid  $\beta$  accumulation after *Porphyromonas gingivalis* infection. *J. Neurochem.* 2020;00:1–13. <https://doi.org/10.1111/jnc.15096>